ADVANCED ELECTRONIC MATERIALS Open Access
www.advelectronicmat.de

Rectification in Ionic Field Effect Transistors Based on Single Crystal Silicon Nanopore

Hao Hong, Xin Lei, Jiangtao Wei, Yang Zhang, Yulong Zhang, Jianwen Sun, Guoqi Zhang, Pasqualina M. Sarro, and Zewen Liu**

Ionic FETs have enormous potential for energy conversion, sensing, and ionic circuits due to their efficient regulation of the nanochannel. Here ionic FETs based on single-crystal silicon nanopores and the rectification of the fabricated devices are studied. The electrical characterization results demonstrated that since the silicon-based nanopores have the advantage of modulating the surface charge due to their semiconductor nature and benefitting from the effective 3D gating effect on the nanochannel, the magnitude and polarity of surface charge can be modulated by the gate voltage. The rectification effect can be adjusted by applying a certain voltage and fulfilling a transition between anion selectivity and cation selectivity when the surface charge polarity is reversed. Moreover, current–voltage characteristics of the reported ionic FET can be switched between ohmic and diode-like regimes. The proposed ionic FETs supply a novel platform to study the ionic properties and have great potential to be applied in large-scale ionic circuits due to their excellent performance. Finally, simulation results prove the surface charge modulated by the gate voltage determines the magnitude and direction of rectification, which is consistent with the reported experiment result.

1. Introduction

Ion channels and nanopores embedded in cell membranes are essential for living organisms since they can maintain normal physiological processes because of their smart functions such as ion selectivity.[1–3] The first biological nanopore used for bio-sensing was in 1996, it reported an ionic current drop when single-stranded DNA passed through the nanopore.[4] Over the past decades, nanochannels and nanopores have emerged as important tools and platforms for various applications. Solid-state nanopores, which complemented the limitations of biological nanopores such as unmodifiable pore size, mechanical, and chemical instability,[5–7] are suggested later. Solid-state nanopores have widely extended applications not only in biotechnology, such as DNA identification[8–10] and protein profiling,[11,12] but also in other fields, which include molecule separation,[13,14] ion-selective,[15,16] power generation,[17] nanopatterning,[18] and nanostencil lithography.[19]

Ionic current rectification (ICR) in nanopores has been extensively explored due to its broad applications including energy conversion, sensing, and ionic circuits.[20] This phenomenon is mainly caused by the asymmetric surface charge distribution and is commonly observed in nanopores with asymmetric structures such as conical nanopores.[21–25] These nanopores manifest preferential conduction of the ionic current, that is, diode-like I-V characteristics.[26–29] Many methods used to regulate the ICR have been reported since the ICR was highly related to the nanopore structure, surface charge, electrolyte species, and pH.[22,30–32] Daiguji et al first introduced a nanofluidic diode to achieve a stronger ICR,[33] and the nanofluidic diode was further explored by Vlassiouk et al later.[34,35] After that, Nam et al introduced an ionic FET based on multiple nanopores with an embedded electrode, the ionic current of the device can be efficiently manipulated by the gate voltage. The results suggested that the ICR in ionic FETs can be regulated by gate voltage.[36] Then Ai et al used a continuum model to comprehensively investigate the ICR in conical nanofluidic FETs and predicted the gate voltage can tune the preferential current direction.[37] Expecting the mentioned devices based on nanopores, the researcher also tried to

H. Hong, G. Zhang, P. M. Sarro
Department of Microelectronics
Delft University of Technology
Delft 2628 CD, The Netherlands
E-mail: p.m.sarro@tudelft.nl
H. Hong, J. Wei, Y. Zhang, J. Sun, Z. Liu
School of Integrated Circuits
Tsinghua University
Beijing 100084, China
E-mail: liuzw@tsinghua.edu.cn
X. Lei
School of Chemistry
Beihang University
Beijing 100084, China
Y. Zhang
School of Electronic and Information Engineering
Beijing Jiaotong University
Beijing 100084, China

The ORCID identification number(s) for the author(s) of this article can be found under https://doi.org/10.1002/aelm.202300782

DOI: 10.1002/aelm.202300782

utilize other strategies to realize effective regulation of the ICR. For example, Cao et al regulated the ICR by applying a salt gradient and explained the ICR caused by the ion concentration difference in asymmetric nanochannels.[38,39] Lin et al utilized the modified surface charge to enable further control of the ICR in nanopores and realized the ICR in large-size nanopores by highly charged surfaces.[40] In addition, many efforts were paid to the controlling pH of the electrolytes and modification of the sidewalls by chemical strategies to implement the regulation of the surface charge.[41–45] However, both acidic and alkaline environments may destroy the structure of the biological molecule to be detected, and the stability and repeatability of chemical modifications also need to be addressed. Thanks to the semi-conductivity of silicon, and benefitting from the effective 3D gating modulation to electrical characteristics of the nanopore channels,[46,47] the ionic FETs based on silicon nanopores are an excellent candidate for several applications such as energy conversion, sensing, and ionic circuits.

In this work, we reported ionic FETs based on single-crystal silicon nanopores, which were obtained by the three-step wet etching (TSWE) method, the gate electrode in the ionic FET was conformed to regulate the surface charge on the nanopore sidewalls. It is worth noting that all the fabrication processes are compatible with the conventional semiconductor and MEMS technology, which indicates the reported device can be fabricated on a large scale at a low cost. With applying a certain gate voltage, the magnitude and polarity of the surface charge can be effectively regulated, as a result, not only the corresponding ICR can be adjusted, but counter-ions enriched in the nanochannel can be switched between cation (K^+) and anion (Cl^-), resulting in a transition between anion selectivity and cation selectivity. Furthermore, the mentioned effective 3D gating can fulfill a switch between ohmic and diode-like current–voltage characteristics of the ionic FET. Finally, the simulation results obtained agree with the measurements of the fabricated devices.

2. Experimental Section

Details of the critical fabrication process steps of ionic FETs based on single-crystal silicon nanopores are schematically exhibited in **Figure 1**. At first, we used photolithography to transfer the patterns of etching windows on the chip. Then inductively coupled plasma (ICP) was utilized to partially remove Si_3N_4 and SiO_2 mask layers to develop the etching windows as depicted in Figure 1b. Next, the anisotropic etching was conducted on both sides of the chip to form the pyramid-shaped pit on the front side and the back large cavity as shown in Figure 1c. After that removal of the buried oxide layer (SiO_2) was carried out by using buffered hydrofluoric acid as exhibited in Figure 1d, later silicon nanopores were prepared by the TSWE method, which is shown in Figure 1e. Finally, a Cr/Au electrode was deposited on the silicon as a gate electrode as shown in Figure 1f and the ionic FET based on a single-crystal silicon nanopore was successfully obtained. To build ohmic contact between the silicon and the Cr/Au electrode, before the deposition of the Cr/Au electrode, the mask layers (both Si_3N_4 and SiO_2) on the electrode were removed by ICP, and the heavy doping of boron was subsequently carried out on the bared silicon by ion implantation with an ion implantation density of 2×10^{15} cm^{-2} and an energy of 30 keV. In the electrical characterization measurement part, oxygen plasma (50 W 10 min) and piranha etch (H_2SO_4:H_2O_2 = 3:1 30 min) were used as the pretreatment to clean the nanochannel and increase its hydrophilicity. Two source meter units (Keithley 2450) were used in the measurement, one for recording the ionic current and the other for applying the gate voltage. Two Ag/AgCl electrodes were used for the drain and the source electrodes. Owing to the polarization or trapping/de-trapping processes, there is a hysteresis in the field effect with the sweep direction of the voltages, the data for all electrical measurements were collected 30 s after the start of the measurement.

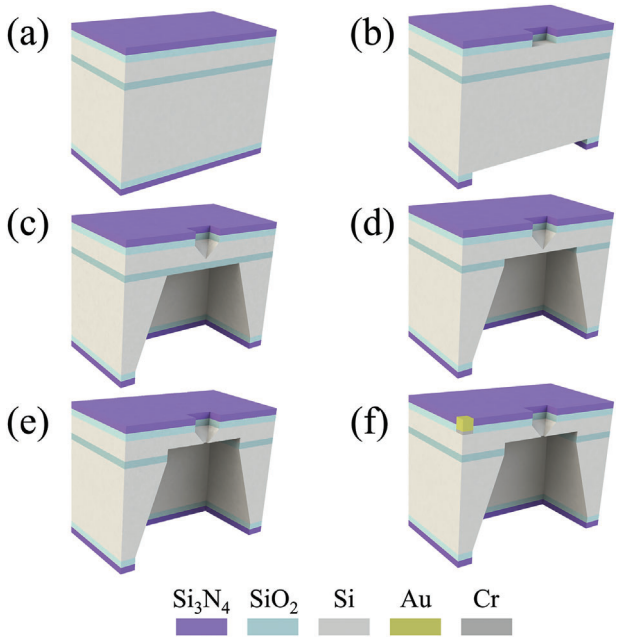

Figure 1. Schematic of the critical fabrication process of the ionic FET based on silicon nanopores. a) Si_3N_4 and SiO_2 mask layers deposition on the SOI wafer b) transfer of patterns by photolithography and removal of mask layers c) formation of pyramid-shaped pit and back etching window d) removal of buried oxide layer e) fabrication of nanopores by TSWE method f) Cr/Au electrode deposition on the silicon.

3. Results and Discussion

Following the above-described process flow, we successfully obtained the ionic FETs based on single-crystal silicon nanopores for the subsequent electrical characterization measurement. First of all, **Figure 2**a shows a cross-sectional-view scanning electron microscope (SEM) image of a pyramid-shaped pit during the preparation process, which corresponds to the fabrication process stage as exhibited in Figure 1c. This square-based pyramid pit with sloped sidewalls was developed by the well-established anisotropic wet etching. Previous reports have demonstrated that the geometry of nanopores including pore size, membrane thickness, and sidewall angle can influence the rectification effect of nanopores.[48] It is well known that controllable fabrication of silicon nanopores of sub-10 nm is challenging on thick silicon membranes by anisotropic wet etching. Thanks to our proposed advanced TSWE method,[49] sub-10 nm nanopores were successfully obtained as shown in Figure S1 (Supporting Information) and Figure 2b where the bottom-view SEM images of nanopores with a feature size of 6 and 10 nm are reported. The result indicates the tremendous potential of the TSWE method for precise and diverse nano-machining.

At first, the electrical characteristics of the obtained ionic FETs without gating were studied. **Figure 3** shows the recorded

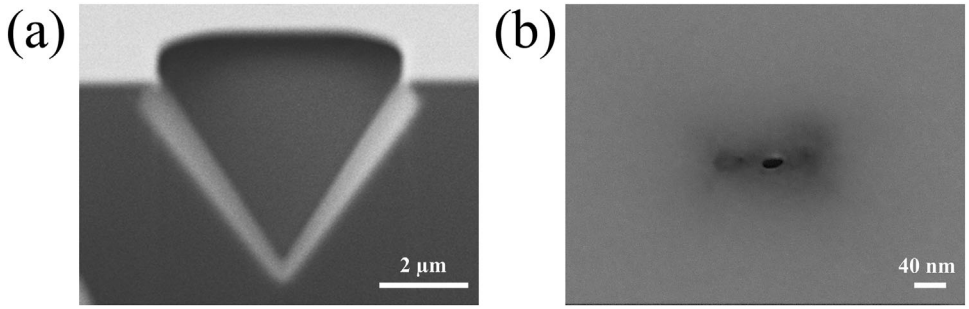

Figure 2. a) A cross-sectional-view SEM image of a front side pit. b) A bottom-view SEM image of a nanopore with a feature size of 10 nm.

current–voltage curves of an obtained ionic FET based on the silicon nanopore with a feature size of 6 nm in different concentrations of the KCl solution. The ionic current increased as the solution concentration increased because higher solution concentrations have higher conductivity, so the conductance throughout the nanochannel increased accordingly, ultimately resulting in the higher ionic current for the same applied bias voltage. Because the ionic current is negligible at 1 mM KCl solution due to the low conductivity, the inset figure gives a separate exhibition of its current–voltage curve. It is worth noting that in higher-concentration KCl solutions, the electrical double layer (EDL) effect can be neglected (Debye length < pore diameter), and the ionic current has a linear relationship with the conductivity of the solution. As the concentration becomes sufficiently dilute, the current reaches saturation and remains virtually constant (Figure S2, Supporting Information). Furthermore, it can be intuitively found that the ionic current recorded at one applied bias voltage is dramatically different from the one at the same magnitude but opposite polarity voltage. At any absolute value of bias voltage, the ionic current is higher at negative voltages ("on" state) than at positive voltage ("off" state), which exhibits ion selectivity and rectification effect.

Then, the ICR of the obtained ionic FETs based on silicon nanopores without gating and factors that affected the ICR of the

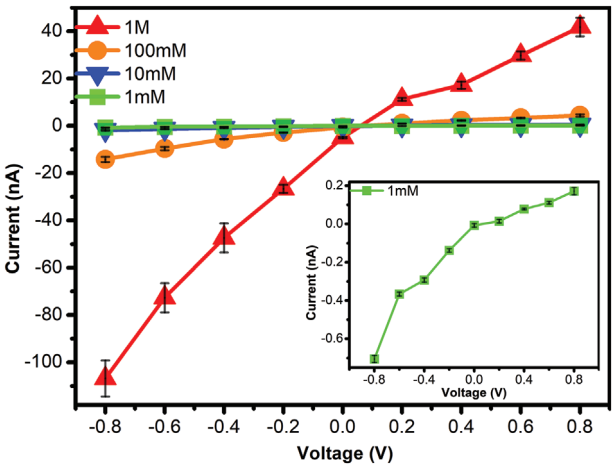

Figure 3. Typical current–voltage curves of an ionic FET based on silicon nanopore with a feature size of 6 nm in KCl electrolyte concentration from 0.001 to 1 M (pH 7.2) and applied bias voltage from −0.8 to 0.8 V.

device were analyzed and discussed. **Figure** 4a shows the rectification factor (RF, $\frac{|i_{-V}|}{|i_{+V}|}$) of different ionic FETs with a feature size of 6, 10, 47, and 72 nm, respectively, in a 1 M KCl solution. As shown in Figure 4a, the stronger ICR was observed in the higher applied bias voltage. A larger applied bias voltage enhances the ion enrichment/depletion in the tip of nanopores, thereby increasing the rectification effect. Theoretical studies confirm that in addition to the cation/anion selectivity decreasing with the increasing ion concentration under a certain voltage, the ion selectivity and ICR are also a function of the applied voltages.[50] Concomitantly, RF gradually increased with the decrease of the pore size. For an applied bias voltage of 0.8 V, the RF of the four ionic FETs with feature sizes of 72, 47, 10, and 6 nm are 1.7, 1.9, 2.2, and 2.6, respectively. The EDL plays a more critical role when the nanopore size steadily decreases and becomes comparable to the Debye length ($\lambda_D = \sqrt{\frac{\varepsilon_0 \varepsilon_r K_B T}{2ne^2}}$, n represents the concentration of the solution), the oppositely charged ions are dominating in the nanochannel so the preferential conduction becomes more intensive, as a result, the smaller sizes of nanopores exhibited a stronger rectification effect. At the same time, the effect of KCl solution concentration on the ICR was studied. Figure 4b shows RF in different solution concentrations of the ionic FET with a feature of 6 nm. Since λ_D is associated with the concentration of the solution, the lower concentration solution requires longer λ_D to counteract the potential caused by the surface charge. As a result, an accumulation of counterions in the nanochannel leads to stronger ion selectivity and ICR. With the solution concentration of 10 mM, RF is 3.8 at an applied bias voltage of 0.8 V. It is worth noting that the EDL almost overlaps the nanochannel under this condition of the solution of 10 mM ($2\lambda_D \approx 6$ nm). On the one hand, more counterions filling the nanochannel will cause a larger ion selectivity and stronger rectification effect than in the higher concentration solution. On the other hand, the ionic current will reach a surface charge-governed region and cause the saturation of the ionic current, because the ionic current contributed by the bulk conductance is negligible after the concentration is <10 mL (Figure S2, Supporting Information). It can be seen from the inset figure in Figure 3 that when KCl solution concentration is 1 mM, the ionic current at positive bias voltage is minimal, and the experimental results obtained may be inaccurate due to the noise of the electrical characterization, so the corresponding rectification results at the lower concentrations are not analyzed here.

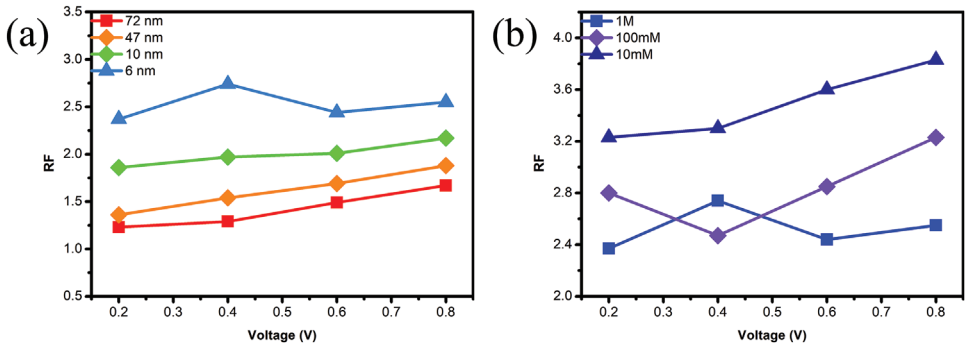

Figure 4. a) RF of the ionic FETs based on silicon nanopores with different feature sizes (1 M KCl solution, pH 7.2) b) RF of the ionic FET based on silicon nanopore with 6 nm feature size in KCl solution (pH 7.2) with different concentrations.

As mentioned before, modulating the surface charge of the nanopores is thought of as a practical approach to effectively regulate the ICR. Here we introduced an ionic FET based on the mentioned silicon nanopores and regulated the ICR by the gate voltage. Due to the semiconductor nature, the nanopores based on single-crystal silicon have the advantage of modulating the surface charge, it is unnecessary to deposit an additional conductive layer. Meanwhile, because the sidewalls of the nanochannel are readily coated by an oxide layer (SiO_2) during the pretreatment (oxygen plasma and piranha etch),[51] the additional insulating layers such as Al_2O_3, HfO_2, and TiO_2 are consequently redundant. This concept of the mentioned device is equivalent to the MOSFET, except that the medium of the nanochannel is replaced by the electrolyte ions in the ionic FET. The unique structure that the ionic nanochannel is surrounded by gate dielectric (SiO_2) allows more efficient 3D gating regulation than other partial gating structures to nanochannel conductivity. **Figure** 5a shows the schematic of the electrical characteristic results with the gate voltage, the gate voltage is transferred to the silicon through the gate electrode. Figure 5b–d reports the recorded current–voltage curves of the ionic FET of 6 nm with different gate voltages in different concentrations of KCl solution (1 M, 100, and 10 mM), respectively. To eliminate the possible current interference caused by leakage dielectric or breakdown, the gate voltage was constantly kept <1.5 V (Supporting Information, Figure S3). It can be found that under the effect of negative gate voltage (red line), the ionic current under the positive bias voltage increases significantly, which agrees with the published results.[36,52] Similarly,

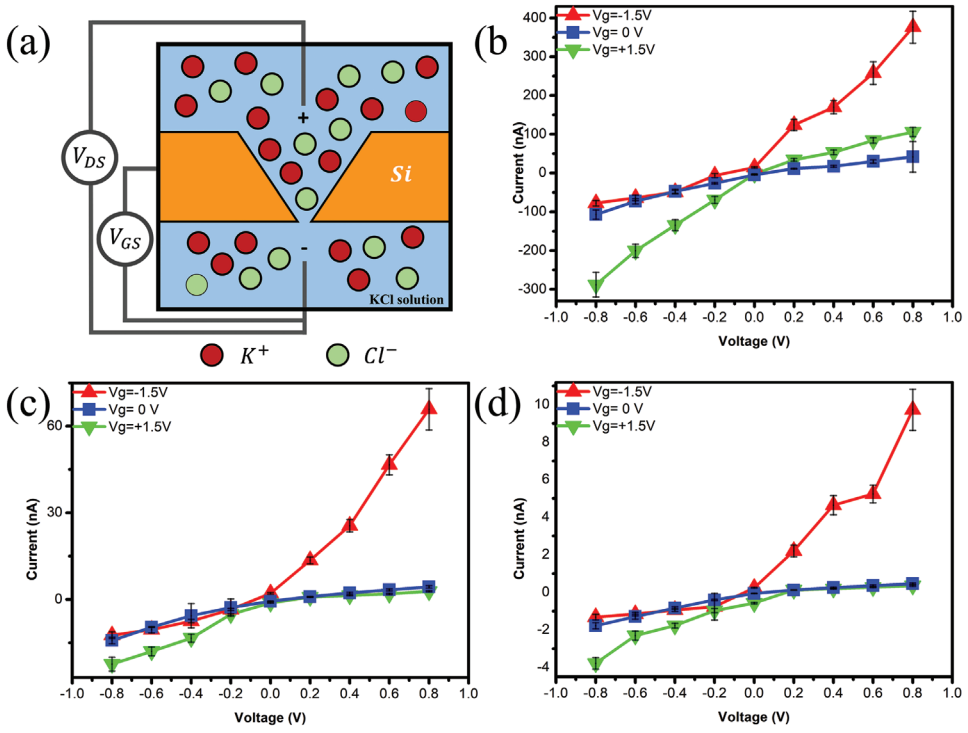

Figure 5. a) Illustration of the ionic FET electric characterization measurement. Typical current–voltage curves of the nanopore-based ionic FET in b) 1 M, c) 100 mM, and d) 10 mM KCl solution (pH 7.2) at different gate voltages.

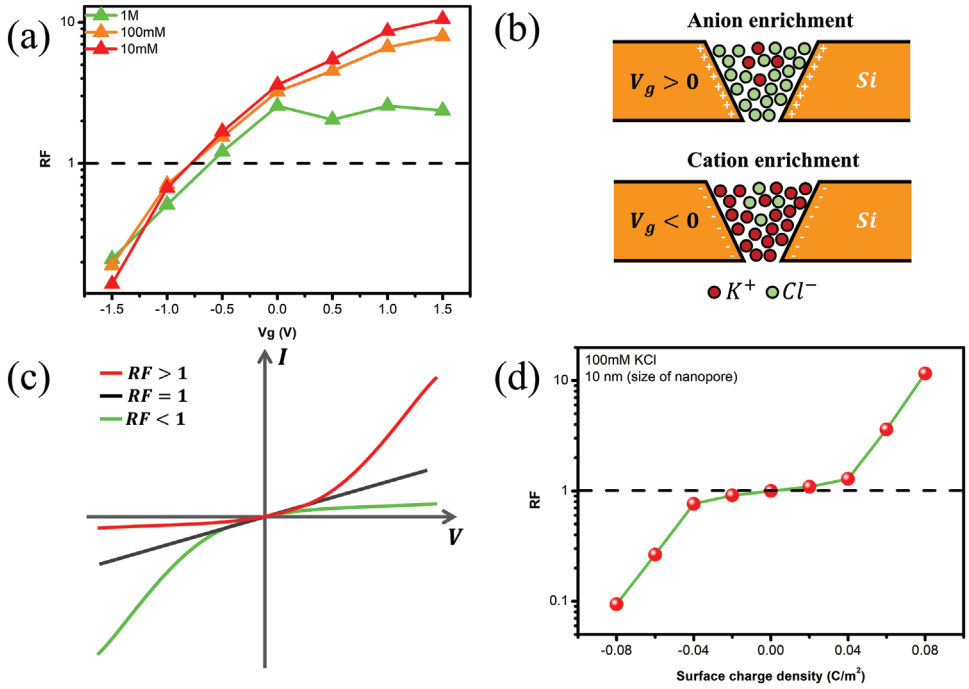

Figure 6. a) Effect of gate voltage on RF of the nanopore-based ionic FET b) Schematic of the majority carrier for the contrary gate voltages (not to scale) c) Schematic diagram of the current–voltage curves corresponding to different RF d) COMSOL simulation result of variation of RF in different surface charge density.

under the effect of positive gate voltage (green line), the ionic current under the negative bias voltage also appears an identical phenomenon (the ionic current under the negative bias voltage increases significantly). The reason for this change in ionic current is considered a result of the enhancement of concentration polarization induced by the gate voltage. It is worth noting that with the gate voltage converted from +1.5 to −1.5 V, a transition from cation selectivity (higher ionic current at negative voltage) to anion selectivity (higher ionic current at positive voltage) appears, and the transition means that the majority carrier in the nanochannel can be switched between cations and anions.

To study the effect of the gate voltage on the ICR of nanopore-based ionic FETs in detail (applied bias voltage is 0.8 V), extracted from Figure 5, the relationship between RF and the gate voltage is plotted in **Figure** 6a. When the gate voltage is 1.5 V, RF corresponding to the three concentrations of KCl solution (10 mM, 100 mM, and 1 M) is 10.5, 8.0, and 2.4, respectively. Obviously, the ability to modulate ICR at lower concentrations is prominent due to the thicker EDL. As mentioned above, without the gate voltage, due to the surface charge present on the nanopore sidewalls, the nanopores exhibited a slight rectification effect, which is consistent with our previous report.[53] For an intuitive understanding of the effect of the gate voltage, the effective surface charge density with gate voltage σ_w^* can be defined as $\sigma_w^* = \sigma_w + \epsilon_o E_g$, where σ_w, ϵ_o, and E_g represented the initial surface charge density (without gate voltage), the permittivity of the nanopore-wall, and the electric field generated by lateral gate voltages at the sidewalls of the nanopore. Determined by the gate voltage, σ_w^* can be regulated in both polarity and magnitude. It indicated that the limitation of the nanopore size by the rectification effect can be broken by a sufficiently high gate voltage and ICR could be enhanced and extended to the larger size nanopores. As shown in Figure 6b, when a positive gate voltage is applied, the electric field effect enhances the influence of the surface charge, leading to greater anion concentration and lower cation concentration. Conversely, under a negative gate voltage, the anions in the nanochannel were decreased and the cations increased, resulting in the different ion selectivity. It is worth noticing that with the gate voltage of ≈−0.75 V, the ionic FET lost the rectification effect (RF = 1), which suggests the nanochannel has no longer ion selectivity, the concentration of anions and cations in the nanochannel is theoretically equal, and the ionic current of the ionic FET followed the ohmic current–voltage characteristics. However, with the increasing of the negative voltage (gate voltage <−0.75 V), the surface charge converts to negative and results in the cations enrichment therefore RF is <1, which indicates that the ion selectivity has switched from cation to anion. As a conclusion, depending on the gate voltage, the ionic current of the prepared ionic FET can be switched between ohmic (RF = 1) and diode-like regimes (RF>1 or RF<1). An illustration of the voltage-current curves for the above three types of RF discussed is schematically shown in Figure 6c. Finally, to verify the surface charge which is regulated by the gate voltage can modulate the ICR. Figure 6d shows the COMSOL simulation result of variation of RF in different surface charge densities (Supporting Information, Simulation description). It can be found that RF is proportional to the gate voltage, and the rectification direction simultaneously changes when the surface charge polarity is reversed, which indicates the ion selectivity changes. Furthermore, when the nanopore sidewalls keep neutral (no net surface charge) the ionic FET has no longer a rectification effect (RF = 1), which is consistent with the experimental data reported.

4. Conclusion

In conclusion, ionic FETs based on single-crystal silicon nanopores were fabricated and investigated. Due to the conductivity of the semiconductor, the magnitude and polarity of the surface charge on the nanopore sidewalls can be effectively manipulated by the gate voltage. As a result, the ionic current of the prepared ionic FET can be switched between ohmic and diode-like regimes, and the rectification can be also adjusted by a certain gate voltage. It is worth noting that the transition between anion selectivity and cation selectivity indicated the switching of the majority carrier between K^+ (hole) and Cl^- (electron), which is equivalent to the P/N-type MOSFET. It can be predicted that if materials with higher permittivity were used as insulating layers, gate voltage could be further increased so the related ionic FETs could achieve a stronger ICR, and the ICR could be extended to nanopores that exceed several hundred times the thickness of EDL, which complemented the limitation of the pore size for various applications. All in all, the proposed ionic FETs supply a novel platform to study the ionic properties and have great potential to be applied in large-scale ionic circuits due to their low-cost fabrication processes and excellent electric performance.

Supporting Information

Supporting Information is available from the Wiley Online Library or from the author.

Acknowledgements

H.H. and X.L. contributed equally to this work. This work was financially supported by The National Key R&D Program (2019YFA0707002), the Beijing Innovation Center for Future Chips, and the Beijing National Research Center for Information.

Conflict of Interest

The authors declare no conflict of interest.

Data Availability Statement

The data that support the findings of this study are available in the supplementary material of this article.

Keywords

Ionic FET, rectification, silicon nanopore, surface charge, gate voltage

Received: November 12, 2023
Revised: April 8, 2024
Published online:

[1] Y. E. Korchev, C. L. Bashford, G. M. Alder, P. Y. Apel, D. T. Edmonds, A. A. Lev, K. Nandi, A. V. Zima, C. A. Pasternak, *FASEB J.* **1997**, *11*, 600.
[2] X. Hou, L. Jiang, *ACS Nano* **2009**, *3*, 3339.
[3] Z. Xu, Z. Zhu, N. Li, Y.e Tian, L. Jiang, *ACS Nano* **2018**, *12*, 10000.
[4] J. J. Kasianowicz, E. Brandin, D. Branton, D. W. Deamer, *Proc. Natl. Acad. Sci.* **1996**, *93*, 13770.
[5] C. Dekker, *Nat. Nanotechnol.* **2007**, *2*, 209.
[6] J. Li, D. Stein, C. McMullan, *Nature* **2001**, *412*, 166.
[7] A. Storm, J. Chen, X. Ling, *Nature Mater* **2003**, *2*, 537.
[8] S. M. Iqbal, D. Akin, R. Bashir, *Nat. Nanotechnol.* **2007**, *2*, 243.
[9] B. M. Venkatesan, R. Bashir, *Nat. Nanotechnol.* **2011**, *6*, 615.
[10] J. Feng, *Nat. Nanotechnol.* **2015**, *10*, 1070.
[11] E. C Yusko, *Nat. Nanotechnol.* **2017**, *12*, 360.
[12] L. Restrepo-Pérez, C. Joo, C. Dekker, *Nat. Nanotechnol.* **2018**, *13*, 786.
[13] F. Montagne, N. Blondiaux, A. Bojko, R. Pugin, *Nanoscale* **2012**, *4*, 5880.
[14] M. L. Kovarik, S. C Jacobson, *Anal. Chem.* **2009**, *81*, 7133.
[15] R. Rollings, A. Kuan, J. Golovchenko, *Nat. Commun.* **2016**, *7*, 11408.
[16] S. Su, Y. Zhang, S. Peng, *Nat. Commun.* **2022**, *13*, 4894.
[17] J. Feng, M. Graf, K. Liu, *Nature* **2016**, *536*, 197.
[18] S. Aksu, *Nano Lett.* **2010**, *10*, 2511.
[19] T. Deng, Y. F. Wang, Q. Chen, H. J. Chen, Z. W. Liu, *Appl. Surf. Sci.* **2016**, *390*, 681.
[20] Y. Q. Fu, H. Tokuhisa, L. A. Baker, *Chem. Commun.* **2009**, *32*, 4877.
[21] Z. Siwy, E. Heins, C. C. Harrell, P. Kohli, C. R. Martin, *J. Am. Chem. Soc.* **2004**, *126*, 10850.
[22] Z. Siwy, *Adv. Funct. Mater.* **2006**, *16*, 735.
[23] J. Cervera, A. Alcaraz, B. Schiedt, R. Neumann, P. Ramírez, *J. Phys. Chem. C* **2007**, *111*, 12265.
[24] H. S. White, A. Bund, *Langmuir.* **2008**, *24*, 2212.
[25] W.-J. Lan, D. A. Holden, H. S. White, *J. Am. Chem. Soc.* **2001**, *133*, 13300.
[26] P. Y. Apel, *Nanotechnology* **2011**, *22*, 175302.
[27] N. Sa, W.-J. Lan, W. Shi, L. A. Baker, *ACS Nano* **2013**, *7*, 11272.
[28] K. P. Singh, *Sens Actuators B Chem* **2016**, *230*, 493.
[29] Y. Dong, Y. Cheng, G. Xu, H. Cheng, K. Huang, J. Duan, D. Mo, J. Zeng, J. Bai, Y. Sun, J. Liu, H. Yao, *ACS Appl. Mater. Interfaces* **2019**, *11*, 14960.
[30] C. Kubeil, A. Bund, *J. Phys. Chem. C* **2011**, *115*, 7866.
[31] M. L. Kovarik, K. Zhou, S. C. Jacobson, *J. Phys. Chem. B* **2009**, *113*, 15960.
[32] J. F. Pietschmann, M. T. Wolfram, M. Burger, C. Trautmann, G. Nguyen, M. Pevarnik, V. Bayer, Z. Siwy, *Phys. Chem. Chem. Phys.* **2013**, *15*, 16917.
[33] H. Daiguji, Y. Oka, K. Shirono, *Nano Lett.* **2005**, *5*, 2274.
[34] I. Vlassiouk, Z. S. Siwy, *Nano Lett.* **2007**, *7*, 552.
[35] I. Vlassiouk, T. R. Kozel, Z. S. Siwy, *J. Am. Chem. Soc.* **2009**, *131*, 8211.
[36] S.-W. Nam, M. J. Rooks, K.i-B. Kim, S. M. Rossnagel, *Nano Lett* **2009**, *9*, 2044.
[37] Y. Ai, J. Liu, B. Zhang, S. Qian, *Sens. Actuators, B* **2011**, *157*, 742.
[38] L. Cao, W. Guo, Y. Wang, L. Jiang, *Langmuir* **2012**, *28*, 2194.
[39] C. Y. Lin, L. H. Yeh, J. P. Hsu, S. Tseng, *Small* **2015**, *11*, 4594.
[40] C.-Y. Lin, L.i-H. Yeh, Z. S. Siwy, *J. Phys. Chem. Lett.* **2018**, *9*, 393.
[41] J.-P. Hsu, S.-T. Yang, C.-Y. Lin, S. Tseng, *J. Colloid Interface Sci.* **2019**, *537*, 496.
[42] M. Liu, H. Zhang, K. Li, L. Heng, S. Wang, Y. Tian, L. Jiang, *Adv. Funct. Mater.* **2015**, *25*, 421.
[43] J.-P. Hsu, Y.-Y. Chu, C.-Y. Lin, S. Tseng, *J. Colloid Interface Sci.* **2019**, *537*, 358.
[44] L. Tshwenya, F. Marken, K. Mathwig, O. A. Arotiba, *ACS Appl. Mater. Interfaces* **2020**, *12*, 3214.
[45] X. Lei, J. Zhang, H. Hong, J. Wei, Z. Liu, L. Jiang, *Small* **2023**, *19*, 2303370.
[46] E. B. Kalman, O. Sudre, I. Vlassiouk, *Anal. Bioanal. Chem.* **2009**, *394*, 413.

[47] G. Laucirica, W. A. Marmisollé, C. Trautmann, O. Azzaroni, *ACS Appl. Mater. Interfaces* **2019**, *11*, 30001.
[48] C. Wen, S. Zeng, S. Li, Z. Zhang, S.-L.i Zhang, *Anal. Chem.* **2019**, *91*, 14597.
[49] H. Hong, J. Wei, X. Lei, *Microsyst Nanoeng* **2023**, *9*, 63.
[50] P. Ramirez, S. Mafe, *Nanotechnology* **2008**, *19*, 315707.
[51] S. Zeng, C. Wen, P. Solomon, *Nat. Nanotechnol.* **2019**, *14*, 1056.
[52] S.-W. Nam, M.-H. Lee, S.-H. Lee, D.-J. Lee, S. M. Rossnagel, K.-B. Kim, *Nano Lett.* **2010**, *10*, 3324.
[53] Y. Wang, Q.i Chen, T. Deng, Z. Liu, *J. Phys. Chem. C* **2018**, *122*, 11516.